



Visualizing Collagen Fibrils in the Cochlea's Tectorial and Basilar Membranes Using a Fluorescently Labeled Collagen-Binding Protein Fragment

Raquel de Sousa Lobo Ferreira Querido¹ · Xiang Ji^{2,3} · Rabina Lakha³ · Richard J. Goodyear⁴ · Guy P. Richardson⁴ · Christina L. Vizcarra³ · Elizabeth S. Olson^{1,2}

Received: 20 September 2022 / Accepted: 16 January 2023

© The Author(s) under exclusive licence to Association for Research in Otolaryngology 2023

Abstract

Purpose A probe that binds to unfixed collagen fibrils was used to image the shapes and fibrous properties of the TM and BM. The probe (CNA35) is derived from the bacterial adhesion protein CNA. We present confocal images of hydrated gerbil TM, BM, and other cochlear structures stained with fluorescently labeled CNA35. A primary purpose of this article is to describe the use of the CNA35 collagen probe in the cochlea.

Methods Recombinant poly-histidine-tagged CNA35 was expressed in *Escherichia coli*, purified by cobalt-affinity chromatography, fluorescence labeled, and further purified by gel filtration chromatography. Cochleae from freshly harvested gerbil bullae were irrigated with and then incubated in CNA35 for periods ranging from 2 h — overnight. The cochleae were fixed, decalcified, and dissected. Isolated cochlear turns were imaged by confocal microscopy.

Results The CNA35 probe stained the BM and TM, and volumetric imaging revealed the shape of these structures and the collagen fibrils within them. The limbal zone of the TM stained intensely. In samples from the cochlear base, intense staining was detected on the side of the TM that faces hair cells. In the BM pectinate zone, staining was intense at the upper and lower boundaries. The BM arcuate zone was characterized by a prominent longitudinal collagenous structure. The spiral ligament, limbus and lamina stained for collagen, and within the spiral limbus the habenula perforata were outlined with intense staining.

Conclusion The CNA35 probe provides a unique and useful view of collagenous structures in the cochlea.

Keywords Tectorial membrane · Basilar membrane · Cochlea · Collagen · Habenula perforata

Introduction

The acellular tectorial membrane (TM) is an accessory structure that spirals along the length of the cochlea. On its medial, modiolar side, the TM is fixed to the apical surfaces

of interdental cells, which form the epithelium overlying the spiral limbus; it then extends laterally, covering the inner and outer hair cells (Fig. 1a, b). Hair bundle deflection is generated by a shearing motion between the reticular lamina and the TM, leading to mechanoelectric transduction [1]. Beyond this most fundamental role, TM mechanics have been hypothesized to be key to producing the cochlea's frequency selectivity [2, 3]. The TM is a gel-like structure that is 97% water and otherwise comprises collagen types II, V, IX, and XI, and noncollagenous glycoproteinsTECTA,TECTB,CEACAM16,OTOG, andOTOGL [4].TECTA,TECTB, andCEACAM16 are the main constituents of the TM striated sheet matrix, within which collagen fibrils are embedded and oriented primarily in the radial direction perpendicular to the cochlear spiral [5, 6].

The TM can be difficult to view *in vivo* and *in vitro* due to its high hydration state and near-transparency and because

✉ Elizabeth S. Olson
eao2004@columbia.edu

¹ Department of Otolaryngology, Head and Neck Surgery, Columbia University, New York, NY, USA

² Department of Biomedical Engineering, Columbia University, New York, NY, USA

³ Department of Chemistry, Barnard College, New York, NY, USA

⁴ Sussex Neuroscience, School of Life Sciences, University of Sussex, Brighton, UK

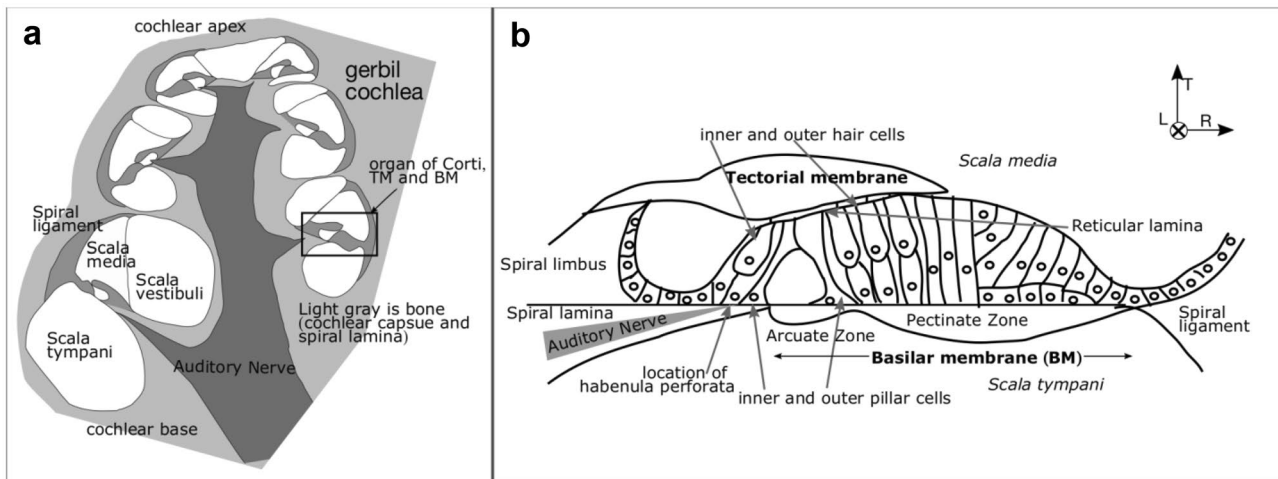


Fig. 1 **a** Sketch of a cross section of the gerbil cochlea, a snail shaped bony capsule enclosing the sensory epithelium. The organ of Corti and tectorial and basilar membranes (TM and BM) coil around a central core, the modiolus, that contains the auditory nerve. Cochlear base and apex are noted. **b** Sketch of the region boxed in (**a**), with the two regions of the BM labeled (arcuate and pectinate zones), and the tectorial membrane shown in its natural position in contact with OHC stereocilia. (In the cartoon, the IHC stereocilia also contact to TM,

although this is uncertain [11].) The location of the hair cells and pillar cells is noted although in our preparations, we did not stain for the cells of the organ of Corti. Auditory neurons extend through the bone of the spiral lamina via the bony holes of the habenula perforata. The longitudinal (L) transverse (T) and radial (R) directions are indicated. Microscopy images (below) are shown in either a radial-longitudinal or an approximate radial-transverse plane

it is an acellular structure that cannot be stained with cell-specific dyes. Second harmonic imaging microscopy (SHIM) was used to image the 3D organization of the collagen fibrils within fresh TM of adult mice [7, 8]. In fixed, dehydrated tissue, the TM has been observed with scanning and transmission electron microscopy (SEM, TEM). These images show the slightly-off-radial orientation of the collagen fibrils and details of the covernet [4, 9]. The imprints of the OHC stereocilia outermost row were observed with SEM, cementing the evidence that the TM and OHC stereocilia are in contact in vivo [9, 10]. In fresh preparations, IHC stereocilia have also been observed to be in contact with the TM [11].

The BM is a fibrous ribbon that supports the organ of Corti. Radially, this ribbon has two sections — the arcuate zone (AZ), which spans from the foot of the inner pillar cell to the foot of the outer pillar cell, and the pectinate zone (PZ), which spans from the outer pillar foot to the spiral ligament (Fig. 1a, b). The BM is composed of collagen type II fibrils [12] in a ground substance that includes the glycoprotein EMILIN2 [13, 14]. The PZ contains orderly radial fibrils; the AZ is less well described in the literature. The shape of the BM varies between species. In the gerbil cochlea, the PZ has a bowed shape, with fibrils on the upper and lower surfaces [15]. The gerbil BM has relatively little longitudinal variation in radial width [16] while in guinea pig and human [17, 18], the BM has a relatively flat shape and a steady increase in width from base to apex. The BM is considered the primary structural element of the cochlear partition [19, 20]. It has been

imaged with electron and light microscopy, in both labeled and unlabeled, and fixed and unfixed preparations [9, 12, 14, 21, 22].

Both the BM and TM are hydrated and suffer from dehydration artifacts, as is apparent when comparing the plump structures imaged from a fresh hemicochlea to the dehydrated structures of histological sections [22]. In the present study, we present confocal images of hydrated gerbil cochleae, stained with a fluorescently labeled collagen-binding protein domain (CNA35). CNA35 binds to the collagen triple helix and has been reported to bind to collagen types I through VI [23]. It is typically used in unfixed tissue and has been used in cell and tissue culture, allowing for visualization of collagen over [23–25].

It is acknowledged that this study was a component of a physiological investigation in which the mechanical properties of the TM were to be manipulated using scala media (SM) injections of collagenase (to reduce stiffness) or polyethylene glycol (to increase viscosity) [26]. However, injection of these agents and ~2 h of in vivo incubation did not result in detectable physiological changes. Because the injections did not induce any apparent changes in the anatomy, this paper presents collagen imaging of hydrated forms of the TM, BM, and other collagenous structures within the cochlea. To our understanding, this is the first use of the CNA35 collagen probe in the cochlea. The imaging reinforced previous findings and resulted in apparently new findings regarding the localization of collagen in the cochlea.

Materials and Methods

CNA35

CNA35 is a fragment of the CNA collagen adhesion protein from *Staphylococcus aureus* bacteria, corresponding to amino acids 30–344, which contain the essential domains for high-affinity collagen binding [27]. The two subdomains of CNA35 (N1 and N2) wrap around the collagen's triple helical structure and make mostly hydrophobic contacts with the glycine/proline/4-hydroxyproline repeats of collagen (Fig. 2; [27]). CNA35 is typically used in unfixed tissue (as in the study here) and it was reported to not bind to denatured collagen [23, 27]. However, a protocol was described for the use of CNA35 in fixed muscle tissue [28].

In our study, BL21-DE3* *Escherichia coli* cells were transformed with a plasmid encoding poly-histidine-tagged CNA35 (from the Maarten Merckx lab in the Netherlands) and grown at 37 °C with 250 rpm shaking in Terrific Broth supplemented with 100 µg/mL ampicillin. When the cells reached an optical density of ≈ 0.6 – 0.9 at 600 nm, the temperature was reduced to 20 °C, and recombinant protein expression was induced with 500 µM isopropyl β -D-1-thiogalactopyranoside (IPTG). After 16 h, cells were harvested by centrifugation, washed with phosphate buffered saline (PBS, 140 mM sodium chloride, 2.7 mM potassium chloride, 10 mM sodium phosphate, 1.8 mM potassium phosphate, pH 7.3), and flash frozen in liquid nitrogen before storing at -80 °C.

For protein purification, all steps were carried out at 4 °C with ice-cold buffers, unless otherwise indicated. Frozen cells (≈ 25 g) were resuspended in extraction buffer (300 mM sodium chloride, 50 mM sodium phosphate pH 8.0, 1 mM β -mercaptoethanol) supplemented with 0.75 mM phenylmethylsulfonyl fluoride and 1.5 µg/mL DNaseI (*Sigma catalog no. DN25*). After lysis by French press, lysates were clarified by centrifugation at $30,000 \times g$ for 40 min.

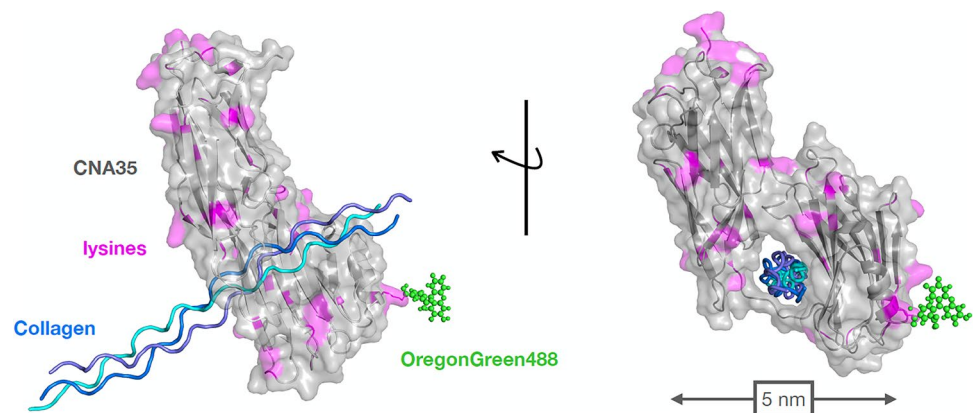
Supernatants were nutated with 1 mL of TALON cobalt-affinity resin (*Takara Bio*). The resin, with bound protein, was washed with 25 mL of extraction buffer, followed by 25 mL of a wash buffer of the same composition with the pH adjusted to 7. Finally, the protein was eluted from the resin with wash buffer supplemented with 200 mM imidazole. The protein was concentrated in an Amicon 10 kDa molecular weight cutoff spin concentrator at $3500 \times g$ and buffer exchanged into 0.1 M sodium bicarbonate.

The CNA35 protein was labeled with succinimidyl esters of either OregonGreen488 (CNA35-OG) or Cy3 (CNA35-Cy3), using a 0.8–5 \times molar excess of dye to protein and nutating at room temperature for 1 h. The reaction was quenched with 20 mM Tris base. The labeled CNA35 was passed through a 0.65 µm Durapore membrane (*Millipore Sigma*) and further purified by gel filtration chromatography on a Superdex200 Increase 10/300GL column (Cytiva) equilibrated with PBS. The concentration of Cy3 was measured at 552 nm using an extinction coefficient of $150,000 \text{ M}^{-1} \cdot \text{cm}^{-1}$. The concentration of OG488 was measured at 496 nm using an extinction coefficient of $72,000 \text{ M}^{-1} \cdot \text{cm}^{-1}$. The concentration of protein was measured at 280 nm using an extinction coefficient of $33,176 \text{ M}^{-1} \cdot \text{cm}^{-1}$ and 280-nm correction factors of 0.12 for OG488 and 0.11 for Cy3. Aliquots of labeled CNA35 were flash frozen in liquid nitrogen and stored at -80 °C. Two batches of CNA35-OG were prepared using this protocol, with labeling of the first batch 57% (from the 0.8:1 molar ratio dye:protein reaction) and of the second batch 135% (from the 5:1 molar ratio dye:protein reaction), where 100% labeling would correspond to one fluorophore per CNA35 molecule. The CNA35-Cy3 was 23% labeled (from the 0.8:1 molar ratio dye:protein reaction).

Gerbil Tissue

Gerbil procedures were approved by the Institutional Animal Care and Use Committee (IACUC) of Columbia University.

Fig. 2 Structural images of CNA35 binding to collagen, created in PyMOL based on PDB code 2F6A. CNA35 binds to unfixed collagen strands in their triple helix form. The CNA35 protein was fluorescently labeled with succinimidyl ester dyes, which covalently modify lysine residues (pink). We are uncertain which of the CNA35 lysines were modified in our labeling protocol. Two possible Oregon Green 488 modifications are shown



The CNA35 staining was done on both ears and was performed post-mortem following in vivo experimental procedures to alter the TM of the left cochlea. These in vivo procedures involved measuring the endocochlear potential (EP) in SM, followed by injection of 0.5–1 μL of either collagenase solution or 8 kDa polyethylene glycol solution. (Examples of EP recordings are in supplemental Fig. 1). To date, the TM modification has not been successful, in that physiological changes have not been noted and staining has not revealed changes in TM structure. At the end of the experiment, both bullae were removed, followed by CNA35 staining, decalcifying, dissecting, and imaging.

Temporal Bone Preparation and Cochlea Dissection

Freshly harvested young adult (approximately 6 months old) gerbil bullae were obtained at the end of physiology experiments. The bullae were opened, middle ear ossicles were removed, and the cochleae were irrigated with 2 μM CNA35 (OG or Cy3, noted in figures below and prepared in PBS) through the oval window. The samples were then immersed in approximately 1.5 mL of the CNA35 solution and stored at room temperature for a duration ranging from 2 h to overnight, following [23]. The cochleae were then fixed in 4% formaldehyde at 4 $^{\circ}\text{C}$, typically for ~24 h and sometimes several days, and subsequently decalcified in ethylenediaminetetraacetic acid (EDTA, 120 mM) for 3 days. The tissue was dissected on a silicone-coated petri dish filled with PBS, and the basal turn was initially separated from the middle and apical turns [29]. One blade of a pair of spring scissors was inserted into the oval window and cuts were made along the lateral wall of the basal turn. The scissors were repositioned by inserting the other blade into the region just cut and the first blade medial to the oval window to isolate the basal turn. Decalcified bony tissue basal to the organ of Corti was removed, and a series of small cuts were made to remove the spiral ligament/lateral wall from the organ of Corti. This is a crucial step because the TM can be accidentally detached from the spiral limbus. To avoid this, the basal turn should be held away from the bottom of the petri dish to prevent deformation, while gentle and precise cuts are made with the scissors, with the plane of the blades at ~a 45 $^{\circ}$ angle with respect to the plane of the organ of Corti. This description applies in cases when the goal was to keep the TM and BM intact and together. This dissection strategy was not always successful, in that in many cases the TM was not retained in place on the limbus. In later dissections, the TM was purposely removed from the limbus and imaged separately from other tissue. Examples from both dissection strategies are shown. Slides were prepared with 1–2 layers of 0.12 mm thick Coverwell Imaging Chambers (EMS 70,327-13S, Hatfield PA). Each dissected section was placed in a drop of Vectashield Antifade mounting medium

(Vector Labs, Burlingame CA) that had been placed in the chamber center. A coverslip was gently applied and attached in place by applying clear nail polish to its rim.

Confocal Microscopy

The dissected turns were imaged on a Nikon A1R laser scanning confocal microscope with a 20 \times air objective lens (0.75 NA/1000 μm WD | CFI60 Plan Apochromat λ) and 20-mW 488-nm Argon-laser to excite OregonGreen488-CNA35. Emission was measured at 525 nm. The 488-nm laser power was set to 2% and the HV-GaAsP detector was set to 20 HV. For the CNA35-Cy3 stained samples, a 561-nm 20-mW diode laser was used for excitation, and emission was measured at 595 nm. Laser power for the 561-nm laser was 4%, and the detector gain was set to 20 HV. Z-stacks were captured spanning 100–150 μm with a step size of 1–2 μm /step. Pixel size was set to 0.62 μm and scanned at a dwell time of 2.3 μs /pixel. The data from confocal laser scanning microscopy were collected through NIS-Elements Advanced Research software and analyzed using the FIJI distribution of ImageJ [30]. Samples were stored in a closed box at 4 $^{\circ}\text{C}$ to avoid exposure to light and dust. The Z-stack projections in the figures are generally maximum intensity projections of a full or partial stack and show radial-longitudinal views. The fluorescent heat maps in the figures are approximately radial-transverse views generated using the “volume viewer” plug-in in FIJI-ImageJ.

Mouse Tissue

An image from a mouse cochlea is included at the end of results. The mouse study was approved by the Sussex University, UK animal welfare committee. The cochlea was from a young adult mouse homozygous for a targeted mutation in which the first coding exon of *Otoa* has been replaced by the sequence encoding EGFP [31]. OTOA is no longer produced in *Otoa*^{EGFP/EGFP} mice, the TM is detached from the spiral limbus, and EGFP is expressed in the interdental cells of the limbus. The mouse was euthanized and the cochleae were harvested and dissected. Dissection and CNA35 labeling were done using HEPES buffered (pH 7.2) Hanks balanced salt solution containing 1 mM Ca²⁺ and 1 mM Mg²⁺. To better maintain the integrity of the interdental cells, the CNA35-Cy3 staining time was carried out on ice for 2 h. The tissue was fixed for an hour, the EGFP signal was amplified with an FITC-anti GFP antibody, and the tissue was then mounted in Vectashield containing DAPI to label the nuclei of the cells. Spiral limbus pieces from the *Otoa*^{EGFP/EGFP} mice were imaged on a Leica SP8 confocal microscope, using a $\times 63$, 1.4 NA oil-immersion lens. Images were captured at 1024 \times 1024, $\times 1.5$ zoom, a line average of 2, and a scan speed 400 Hz.

We include a second figure from a mouse study as supplemental Fig. 2. This was a mouse cochlea from a just-euthanized mouse from the Columbia University animal facility (euthanized within the facility, as part of a tissue-use program). This study was done for training purposes, and the imaging results were useful regarding penetration of the CNA35 dye into the BM. Processing was like that for gerbil, with 2 h staining with CNA35-OG, followed by fixation, decalcification, dissection, and imaging.

Results

To visualize collagen in the gerbil cochlea, we irrigated and incubated intact, unfixed cochleae with fluorescently labeled CNA35, followed by fixation, dissection, and confocal imaging. As noted, some of the gerbil preparations had been treated with intra-SM injections of agents to perturb the TM; however, perturbation has not been successful to date. Both untreated and treated preparations are included in this imaging study and, although this status did not influence the results, it is indicated in Table 1.

In the specimen of Fig. 3a, b, the anatomical structure was maintained during the dissection allowing TM and BM to be visualized together. Their relative orientation is seen in the approximate radial-transverse heat map of Fig. 3a. The limbal zone of the TM in Fig. 3a, b stains particularly brightly, and the fibrils of the TM are clear in the radial-longitudinal view of Fig. 3b (see Fig. 1b for orientation). The BM staining was not as bright as the TM, and brightening the image (such that the TM appears saturated) made the fibrils of the BM visible (inset in Fig. 3b). The TM and BM fibrils are angled differently — the TM fibrils slant toward the apex relative to the fibrils of the BM. The approximate radial-transverse heat maps in Fig. 3a, c highlight the upper and lower bands of collagen fibrils in the PZ of the BM [15, 32]. The specimen of Fig. 3c, d was imaged from the scala tympani (ST) side and additional regions of the BM and limbus are visualized, whereas the TM was not visualized and might have lifted off the structure. In the Z-stack projection

of Fig. 3d, the BM PZ shows orderly radial fibrils, while the AZ of the BM is dominated by relatively thick longitudinal bands that appear bright in the heat map (asterisks in c and d). Capillaries within the limbus are apparent in Fig. 3c, d (arrows in d).

In the sample of Fig. 4, the TM became detached from the limbus during dissection, and the image is of the spiral ligament, BM, spiral lamina, and spiral limbus. The sample was placed on the slide so that the SM side was closer to the imaging optics than the ST side, favoring the imaging on the SM side. In the radial-longitudinal view (Fig. 4b), the PZ shows thin, orderly radial fibrils, while the anatomy of the AZ is dominated by two relatively thick longitudinal bands (asterisks). The habenula perforata (HP) in the spiral lamina are brightly outlined by fluorescence and are visible as the bright bisected circle in the fluorescent heat map (Fig. 4a), indicating that this collagenous lining of the HP spanned the width of the spiral lamina. The spiral ligament and surface of the spiral limbus stain brightly. The region of the interdental cells of the limbus is particularly bright and snake-like in Fig. 4b. The bright regions are extracellular matrix surrounding the interdental cells. (A murine sample shown in Fig. 7 is also useful for parsing this anatomy.) The brightness indicates a high density of collagen in the extracellular matrix of the limbus.

Figure 5 shows a confocal Z-stack in different layers and views. The volumetric view in Fig. 5a appears as an intact cochlear partition (minus the cells of the organ of Corti, which would not have stained (see supplemental Fig. 3). The fluorescent heat map in Fig. 5a' shows the same features as the heat maps of Figs. 3 and 4: bright fluorescence in the limbal region of the TM and the limbus, in the upper and lower layers of BM PZ fibrils, and circling the HP. A projection of the full Z-stack is shown in Fig. 5b, while projections from subsets of the Z-stack showing the TM region are in Fig. 5c, c', c'', and of the BM region are in Fig. 5d, d', d''. Figure 5c, a single slice from the apical side of the TM, shows the TM attachment to the interdental cells of the spiral limbus. Figure 5c', 20 μm deeper, shows a dark separation between the limbus and the TM, due to the anatomical indentation in the TM that

Table 1 Gerbil cochlea specimens presented in this report. More information on the CNA stains is in the “Materials and Methods” section. SM, scala media; PEG, polyethylene glycol; CNA35-OG, CNA35 labeled with OregonGreen488; CNA35-Cy3, CNA35 labeled

with Cyanine3. The imaging reported in this study was not apparently influenced by the PEG and collagenase injections; the information in the table is included for completeness

Animal, figure #	Dye and duration of incubation with dye	Notes
g901, Fig. 3	CNA35-OG, 57% labeled batch, 2 h	Left ear. No collagenase or PEG used. No injection into SM
g924, Fig. 4	CNA35-Cy3, overnight	Right ear. No injection into SM
g932, Fig. 5	CNA35-OG, 135% labeled batch, overnight	Left ear. PEG injection into SM
g941, Fig. 6	CNA35-OG, 135% labeled batch, overnight	TM purposely separated from limbus. Left cochlea had collagenase injection into SM. Both left and right ear TM shown

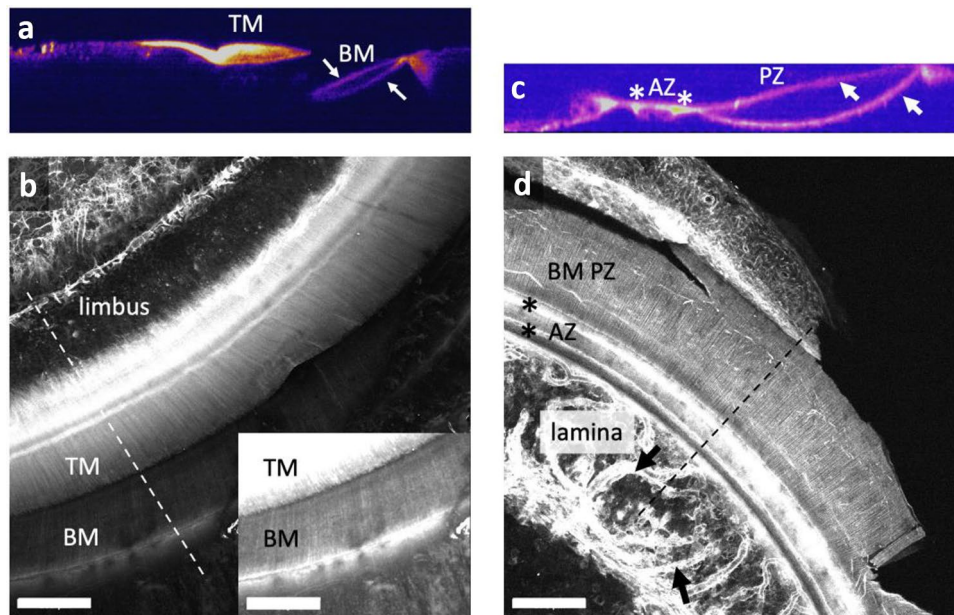


Fig. 3 CNA35-OG staining in a cochlea with no SM injection. **a** and **b** Basal turn. The fluorescence heat map in **(a)** is an approximately radial-transverse view from the location indicated by the dashed line in **(b)**. Staining intensity increases blue: purple: pink: orange: white. **b** A projection of the Z-stack gives a radial-longitudinal gray scale image. The inset is a copy of the lower left portion of the stack, brightened to show the BM more clearly. TM, BM, and spiral limbus are labeled. Arrows in **(a)** indicate the bands of collagen fibrils in the pectinate zone (PZ) of the BM. **c** and **d** Middle turn. A second sample from the same cochlea was positioned on the slide upside-down

relative to **(a)** and **(b)**, so that the scala tympani (ST) side was more brightly imaged than the SM side. The fluorescence heat map in **(c)** is an approximately radial-transverse view from the location indicated by the dashed line in **(d)**. Staining intensity increases blue: pink: white. Only the BM is visible (the TM might have detached). A projection of the Z-stack gives the radial-longitudinal gray scale image in **(d)**. Asterisks indicate longitudinal bands in the BM's arcuate zone (AZ). Arrows in **(c)** indicate the bands of fibrils in the BM PZ. Black arrows in **(d)** indicate capillaries within the lamina. All scale bars are 100 μm

is clear in the volumetric and approximate radial-transverse views of panels **a** and **a'** (arrow in **a'**). In the BM slice of Fig. 5d, in addition to the BM fibrils, the CNA35 dye stained the spiral ligament and outlined the HP of the spiral lamina. A prominent longitudinal cord-like band is observed in the BM AZ in Fig. 5d', 10 μm deeper than in Fig. 5d. A subtle yet clear longitudinal band appears in the PZ region of the BM (arrows in Fig. 5d, d"). This longitudinal feature is also evident in Fig. 5a and might relate to the boundary between the BM and the organ of Corti. A similarly located longitudinal structure was observed in decellularized cochleae [33]. The right-most images (Fig. 5c", d") are projections from the TM and BM regions, respectively. The TM fibrils slant towards the apex relative to the radial BM fibrils. The BM fibrils appear anchored on both sides of the PZ, at the spiral lamina and the lateral edge of the AZ, where the outer pillar foot would be (Fig. 1b).

Intentionally isolated TMs are shown in Fig. 6. The approximately radial-transverse heat maps of fluorescence emphasize the density of the collagen fibrils in the limbal region where the TM would connect to the limbus. Apparent in the heat maps is that the structure of the gelatinous, water-dominated TM structure retains its shape when detached,

with a plump, wing-shaped TM body and narrow extension that would have been attached to the limbus. The gray scale projections show the off-radial slant of the collagen fibrils, particularly clear in Fig. 6c in which the TM retains its longitudinal arc, and the fibrils are oriented with a slant relative to the radial direction. There is a bright region in what would have been the hair-cell facing underside of the TM observed in both the heat map and gray scale projection from the basal turn TM of Fig. 6c. This region appears to be the shell-like structure that was noted in the basal TM of mouse [7].

The SM of the left cochlea in Fig. 6b, c was injected with collagenase, but with no apparent change to the physiology. These TM images, showing middle-turn TM from both right (Fig. 6a) and left (Fig. 6b) cochleae, show no left–right differences, consistent with the apparent ineffectiveness of our collagenase treatment to-date.

Control Image from a Transgenic Mouse

To explore the prominent CNA35 staining within the spiral limbus, we did a study in mouse, in which the cellular and extracellular tissues in the limbus were delineated by means

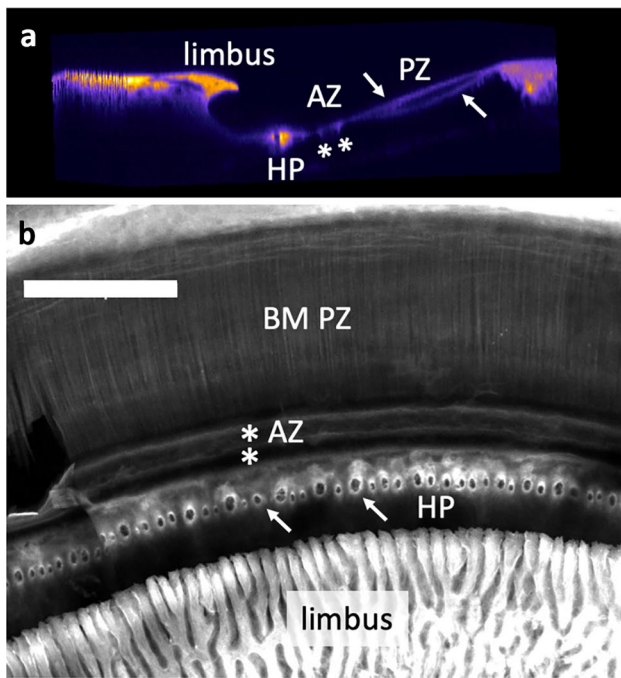


Fig. 4 CNA35 staining in a cochlea with no SM injection. Basal turn. TM was removed during dissection. The fluorescence heat map in (a) is an approximately radial-transverse view. Staining intensity increases blue: purple: orange: yellow. Arrows in (a) indicate the bands of collagen fibrils in the BM PZ. Asterisks in (a) and (b) indicate the longitudinal bands in the BM AZ. A projection of the Z-stack gives the radial-longitudinal gray scale view in (b). The habenula perforata (HP) are outlined by fluorescence (arrows indicate two of many). Scale bar = 100 μ m

of fluorescent labeling. In Fig. 7a-c, we show triple-labeling for GFP that is expressed in the cytoplasm of the interdental cells of the limbus in the *Otoa^{EGFP/EGFP}* knockin-knockout mice (green), for collagen fibrils with CNA35-Cy3 (red), and for nuclear DNA with DAPI (blue). Because the TM detaches from the organ of Corti in *Otoa^{EGFP/EGFP}* mice, this image is of the spiral limbus without the TM. The flask-shaped interdental cells (green) are surrounded by CNA35-stained collagenous extracellular matrix (red). The separation is most clearly seen in the view afforded by Fig. 7c. This control preparation affirms that the intense CNA35 staining we observed in the gerbil limbus is collagen in the extracellular matrix.

Discussion

The present study used a fluorescently labeled collagen-binding protein (CNA35) to visualize the organization of collagen fibrils within the TM, BM, and other regions of the cochlea. The dye was applied to unfixed tissue for a duration of 2 h or overnight (Table 1), with both durations resulting in

successful staining. Following staining, the tissue was fixed, but due to the long period of time staining at room temperature, the status of the cells of the organ of Corti is assumed to be somewhat degraded, although we did not routinely counterstain to visualize cells. (See supplemental Fig. 3 for an indication of how the hair cells in cochlear cultures appear after similar periods of incubation prior to fixation.) The tissue remained hydrated throughout and was imaged with confocal microscopy.

The CNA35-based collagen probe allowed for clear visualization of the TM and BM radial fibrils. In some cases, the relative positions of the TM, BM, and spiral lamina, limbus, and ligament were retained, allowing for visualization of this full structure. The outlines of the HP, the bony holes where auditory nerve fibrils would emerge from the spiral lamina to contact hair cells, were brightly stained. Observing individual slices in a Z-stack allowed for visualization of the TM attachment to the interdental cell region of the spiral limbus (Fig. 5c). The spiral limbus and ligament stained brightly and are known to contain collagen [21, 34].

The TM maintained its plump, wing-like shape following dissection and the TM collagen fibrils displayed their previously documented off-radial slant [4, 9]. A shell-like structure on the hair-cell-facing surface of the TM, similar to that described by Gueta et al. [7] in the basal half of the mouse cochlea, is highlighted by CNA35 staining in the basal-turn image of Fig. 6c. While similar staining is not visible in Figs. 3a and 5a', these images are from intact BM + TM samples in which the extreme basal end of the cochlea was unlikely to be present, due to dissection challenges. As it is only the basal 15% of the gerbil cochlea (in contrast to 40% of the mouse cochlea) that responds to frequencies > 30 kHz [35, 36], the collagen-rich shell-like structure may be a high-frequency specialization of Kimura's membrane, a structure on the surface of the TM into which the hair-cell stereocilia are embedded [37].

The intense CNA35 staining in the TM's limbal zone indicates dense collagen in that region. This apparently stiff cantilever-like attachment region of the TM would provide a rigid support for the TM body, which will impact the shearing motion between the reticular lamina and TM that leads to hair cell excitation (Fig. 1b). Recent measurements of sound-induced motions in freshly excised gerbil cochleae found that the TM rotated in a manner between that of a limbus-attached rigid body and a detached fluid body [38]. The imaging here is in harmony with that finding, with a densely collagenous, and thus relatively rigid limbal region and a less densely collagenous, more fluid TM body.

The collagen staining in the BM PZ was more intense in bands at the upper and lower boundaries than in the middle of the BM. These fibril bands have been described in gerbil [15] and their mechanical impact explored in computational models [32, 39]. (In this article's supplemental Fig. 2,

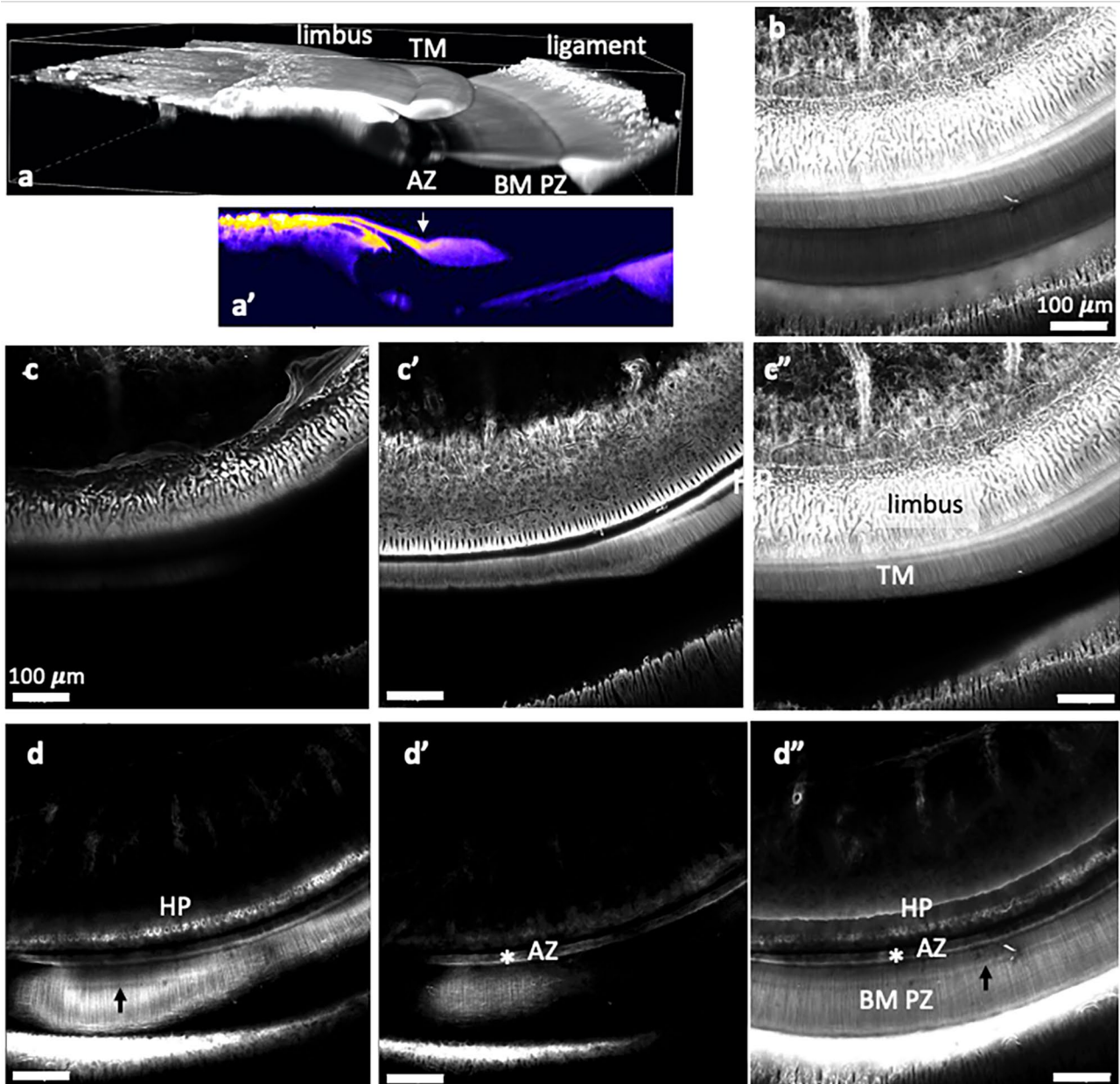


Fig. 5 CNA35 staining in a cochlea with SM injection of polyethylene glycol (PEG). Basal turn. The PEG injection did not cause a notable change in physiology and the anatomy also appeared unchanged due to the injection (compare with Fig. 3). The anatomical structure was maintained during the dissection process allowing TM and BM to be visualized together. **a** Volumetric view. **a'** Fluorescent heat map with approximately radial-transverse view. Staining intensity increases blue: pink: yellow. **b** Full Z-stack projection. **c**, **c'**, **c''** Slices emphasizing the TM layer of the Z-stack. The Z-slice resolution was

2 μm . There was a separation of 20 μm between (**c**) and (**c'**); (**c''**) is a projection of the TM region. **d**, **d'**, **d''** Slices emphasizing the BM layer of the Z-stack. There is a separation of 10 μm between (**d**) and (**d'**); (**d''**) is a projection of the BM region. The asterisks in (**d'**) and (**d''**) indicate the longitudinal bands in the BM AZ. Black arrows in (**d**) and (**d''**) identify a subtle longitudinal band in PZ. White arrow in (**a'**) is an indentation that produces the black band between the limbus and the TM in (**c'**). All scale bars are 100 μm

CNA35 staining in a mouse cochlea is shown and does not show the two-banded structure. The supplemental figure is included to support that the observed bands are not an artifact of poor dye penetration.) In contrast to the expected collagen distribution in the BM PZ, an unexpected finding

was that the AZ of the BM was characterized by a prominent longitudinal structure. Anatomical studies in mustached bat showed a similar longitudinal structure in the BM AZ, and the authors suggested it was a remnant of a spiral blood vessel [40]. That suggestion is consistent with the appearance

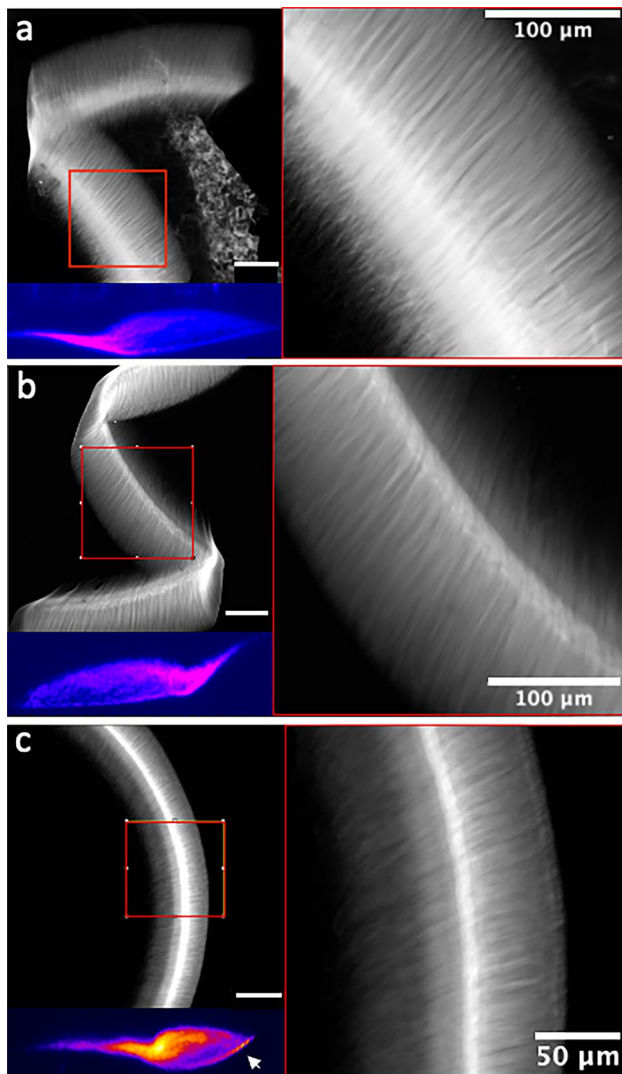


Fig. 6 CNA35 staining of the isolated TM. **a** Middle turn TM from right cochlea, which did not receive a SM injection. **b** and **c** Middle and basal turns respectively, from left cochlea in which collagenase had been injected into the SM. No physiological or anatomical changes due to the collagenase were noted. The fluorescent heat maps are approximate radial-transverse views; the gray-scale projections are radial-longitudinal views. The limbus side of the TM is on the left in the heat maps of **(a)** and **(c)**, and on the right in **(b)**. Scale bars on the left are all 100 μm . The regions within the red boxes on the left side are expanded on the right side of the figure. In **(c)**, a shell-like surface structure is identified with an arrow. Staining intensity progresses blue:pink in **(a)** and **(b)**, blue:pink:orange:yellow in **(c)**

of the structure in our studies. Whether this longitudinal collagenous structure impacts cochlear mechanics is not known. It might confer longitudinal coupling, which is important in some cochlear models [41–43]. It is notable that in point stiffness measurements across the gerbil BM, the AZ was more compliant than the PZ [44]. This is consistent with the

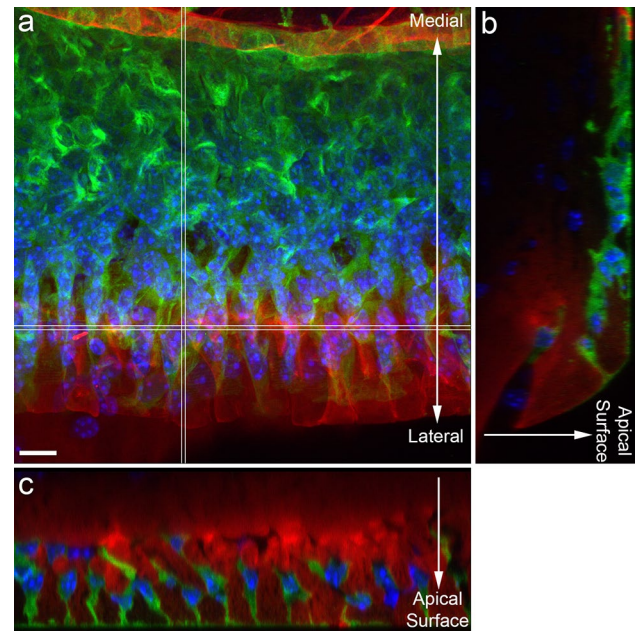


Fig. 7 Region of spiral limbus from an *Otoa*^{EGFP/EGFP} mouse. **a** Z-stack projection. **b** and **c** Perpendicular views of the Z-stack from the regions indicated by the vertical **(b)** and horizontal **(c)** double white lines in **(a)**. The red collagen staining (CNA35-Cy3) is separate from the flask shaped interdental cells (green EGFP staining with blue DAPI-stained nuclei). This separation is particularly clear in **(b)** and **(c)**. Scale bar = 10 μm

longitudinal AZ structure being a remnant of a blood vessel, which could be relatively compressible for a point load.

The intense staining of the HP fully spanned the spiral lamina, appearing as a lining for each individual HP. This ring of collagenous material is reminiscent of the annulus fibrosus of the intervertebral disc [45], where a collagenous ring resists expansion when the disc is compressed. In the case of the HP, the dense collagen ring might serve to resist expansion or contraction of the opening to maintain the size of individual HP.

In conclusion, confocal imaging using the CNA35 probe can be used to study collagen-fibril distribution in fully hydrated and unfixed extracellular matrices of the cochlea that play key roles in frequency tuning. It requires simpler and more readily available equipment than SHIM and, like SHIM [8] may prove to be a valuable tool for studying the collagen fibril distribution in the cochlea of different mouse mutants. The images we show revealed the presence of a longitudinal cord-like structure within the BM AZ in the gerbil and confirm the shell-like appearance of the hair-cell facing TM surface in the cochlear base. These are little-noted aspects of cochlear anatomy that may be significant to cochlear mechanics.

Supplementary Information The online version contains supplementary material available at <https://doi.org/10.1007/s10162-023-00889-z>.

Acknowledgements This work was supported by R01 DC015362 from the National Institute of Deafness and Communication Disorders, the Emil Capita Foundation, Barnard College Summer Research Institute, and by the Biotechnology and Biological Sciences Research Council (BBSRC) (BB/T016337/1). The confocal microscope used in this study was purchased with funds from the National Science Foundation, Division of Biological Infrastructure (MRI grant #1828264).

Data Availability Image files in nd2 format are available upon request.

Declarations

Conflict of Interest The authors declare no competing interests.

References

- Davis H (1958) A mechano-electric theory of cochlear action. *Ann Otol Rhinol Laryngology* 67:789–801
- Lamb JS, Chadwick RS (2011) Dual traveling waves in an inner ear model with two degrees of freedom. *PRL* 107(088101):1–4
- Nankali A, Wang Y, Strimbu CE, Olson ES, Grosh K (2020) A role for tectorial membrane mechanics in activating the cochlear amplifier. *Sci Rep* 10(17620):1–15
- Goodyear RJ, Lu X, Deans MR, Richardson GP (2017) A tectorin-based matrix and planar cell polarity genes are required for normal collagen-fibril orientation in the developing tectorial membrane. *Development* 144:3978–3989
- Killick R, Legan PK, Malenczak C, Richardson GP (1995) Molecular cloning of chick β -tectorin, an extracellular matrix molecule of the inner ear. *J Cell Biol* 129:535–547
- Legan PK, Lukashkina VA, Goodyear RJ, Kössl M, Russell IJ, Richardson GP (2000) A targeted deletion in α -tectorin reveals that the tectorial membrane is required for the gain and timing of cochlear feedback. *Neuron* 28:273–285
- Gueta R, Tal E, Silberberg Y, Rouso I (2007) The 3D structure of the tectorial membrane determined by second-harmonic imaging microscopy. *J Structural Bio* 159(1):103–110
- Gueta R, Levitt J, Xia A, Katz O, Oghalai JS, Rouso I (2011) Structural and mechanical analysis of tectorial membrane tecta mutants. *Biophys J* 100:2530–2538
- Lim DJ (1972) Fine morphology of the tectorial membrane: its relationship to the organ of Corti. *Arch Otolaryngology* 96:199–215
- Kimura RS (1966) Hairs of the cochlear sensory cells and their attachment to the tectorial membrane. *Acta Oto Laryngologica* 61:55–72
- Hakizimana P, Fridberger A (2021) Inner hair cell stereocilia are embedded in the tectorial membrane. *Nature Comm* 12:2604
- Dreiling FJ, Henson MM, Henson OW Jr (2002) The presence and arrangement of type II collagen in the basilar membrane. *Hear Res* 166:166–180
- Amma LL, Goodyear R, Faris JS, Jones I, Ng L, Richardson G, Forrest D (2003) An emilin family extracellular matrix protein identified in the cochlear basilar membrane. *Mol Cell Neurosci* 23(3):460–472
- Russell IJ, Lukashkina VA, Levic S, Cho Y-W, Lukashkin AN, Ng L, Forrest D (2020) Emilin 2 promotes the mechanical gradient of the cochlear basilar membrane and resolution of frequencies in sound. *Sci Adv* 6(eaba2634):1–13
- Schweitzer L, Lutz C, Hobbs M, Weaver SP (1996) Anatomical correlates of the passive properties underlying the developmental shift in the frequency map of the mammalian cochlea. *Hear Res* 97:84–94
- Plassman W, Peetz W, Schmidt M (1987) The cochlea in gerbilline rodents. *Brain Behav Evol* 30:82–102
- Wada H, Sugawara M, Kobayashi T, Hozawa K, Takasaka T (1998) Measurement of guinea pig basilar membrane using computer-aided three-dimensional reconstruction system. *Hear Res* 120:1–6
- Liu W, Atturo F, Aldaya R, Santi P, Cureoglu S, Obwegeser S, Glueckert R, Pfaller K, Schrott-Fisher A, Rask-Andersen H (2015) Macromolecular organization and fine structure of the human basilar membrane - relevance for cochlear implantation. *Cell Tissue Res* 360:245–262
- Steele CR (1972) Behavior of the basilar membrane with pure-tone excitation. *JASA* 55:148–162
- Olson ES, Mountain DC (1991) In vivo measurement of basilar membrane stiffness. *JASA* 89:1262–1274
- Tsuprun V, Santi P (1999) Ultrastructure and immunohistochemical identification of the extracellular matrix of the chinchilla cochlea. *Hear Res* 129:35–49
- Edge RM, Evans BN, Pearce M, Richter CP, Hu X, Dallos P (1998) Morphology of the unfixed cochlea. *Hear Res* 124:1–16
- Krahn KN, Bouten CVC, Van Tuijl S, Van Zandvoort MAMJ, Merckx M (2006) Fluorescently labeled collagen binding proteins allow specific visualization of collagen in tissues and live cell culture. *Anal Biochem* 350:177–185
- Aper SJ, van Spreuwel AC, van Turnhout MC, van der Linden AJ, Pieters PA, van der Zon NL, de la Rambelje SL, Bouten CV, Merckx M (2014) Colorful protein-based fluorescent probes for collagen imaging. *PLoS ONE* 9(12):e114983
- Rubbens MP, Driessen-Mol A, Boerboom RA, Koppert MMJ, van Assen HC et al (2009) Quantification of the temporal evolution of collagen orientation in mechanically conditioned engineered cardiovascular tissues. *Ann Biomed Eng* 37:1263–1272
- Sellon JB, Ghaffari R, Farrahi S, Richardson GP, Freeman DM (2014) Porosity controls spread of excitation in tectorial membrane traveling waves. *Biophys J* 106:1406–1413
- Zong Y, Xu Y, Liang X, Keene DR, Höök A, Gurusiddappa S, Höök M, Narayana SVL (2005) A “Collagen Hug” model for *staphylococcus aureus* CNA binding to collagen. *EMBO J* 24:4224–4236
- Mohammadkhah N, Simms CK, Murphy P (2017) Visualisation of collagen in fixed skeletal muscle tissue using fluorescently tagged collagen binding protein CNA35. *J Mech Behav Biomed Mater* 66:37–44
- Montgomery SC, Cox BC (2016) Whole mount dissection and immunofluorescence of the adult mouse cochlea. *J Vis Exp* 107:e53561
- Schindelin J, Arganda-Carreras I, Frise E et al (2012) Fiji: an open-source platform for biological-image analysis. *Nat Methods* 9:676–682
- Lukashkin AN, Legan PK, Weddell TD, Lukashina VA, Goodyear RJ, Welstead LJ, Petit C, Russell IJ, Richardson GP (2012) A mouse model for human deafness DFNB22 reveals that hearing impairment is due to a loss of inner hair cell stimulation. *PNAS* 109:19351–19356
- Kapuria S, Steele CR, Puria S (2017) Unraveling the mystery of hearing in gerbil and other rodents with an arch-beam model of the basilar membrane. *Sci Rep* 7:228
- Santi PA, Aldaya R, Brown A, Johnson S, Stromback T, Cureoglu S, Rask-Andersen H (2016) Scanning electron microscopic examination of the extracellular matrix in the decellularized mouse and human cochlea. *JARO* 17:159–171
- Slepecky NB, Savage JE, Cefaratti LK, Yoo TJ (1992) Electron-microscopic localization of type II, IX, and V collagen in the organ of Corti of the gerbil. *Cell Tissue Res* 267:413–418

Three supplemental figures for **Visualizing collagen fibrils in the cochlea's tectorial and basilar membranes using a fluorescently labelled collagen-binding protein fragment.**

Supplemental Figure 1. Endocochlear potential (EP) and cochlear injections.

As described in the main article, some of the cochleae used in this study were treated with injections of collagenase or polyethylene glycol (PEG) into scala media. While the injections were performed to change tectorial membrane mechanics, robust, interesting changes have not been noted in physiology or anatomy. This supplemental information is included for completeness.

EP and injection methods: The EP was measured through an approximately 10 μm diameter hole in the scala media of the second turn of the cochlea, using a glass microelectrode with a $\sim 8 \mu\text{m}$ tip and a resistance of $\sim 8 \text{ M}\Omega$. The electrode was filled with a solution of 8 kDa polyethylene glycol (10 mM) in artificial endolymph (KHCO_3 25 mM + KCl 140 mM). The electrode was connected to a microelectrode holder (MPH6R, WPI), with a silver /silver chloride wire within, allowing EP measurement. A 10 μL Hamilton syringe, filled with the artificial endolymph solution was attached to the MPH6R connector. This entire circuit was coupled to a micropump (WPI) programmed to inject $\sim 50 \text{ nL/min}$ for 10 minutes (total of 500 nL per cycle).

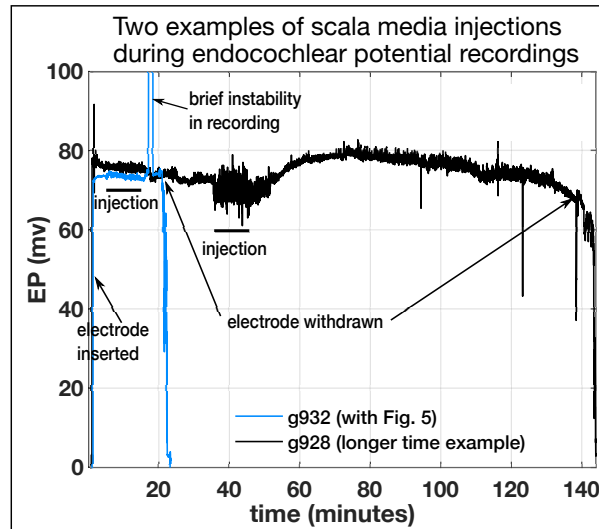


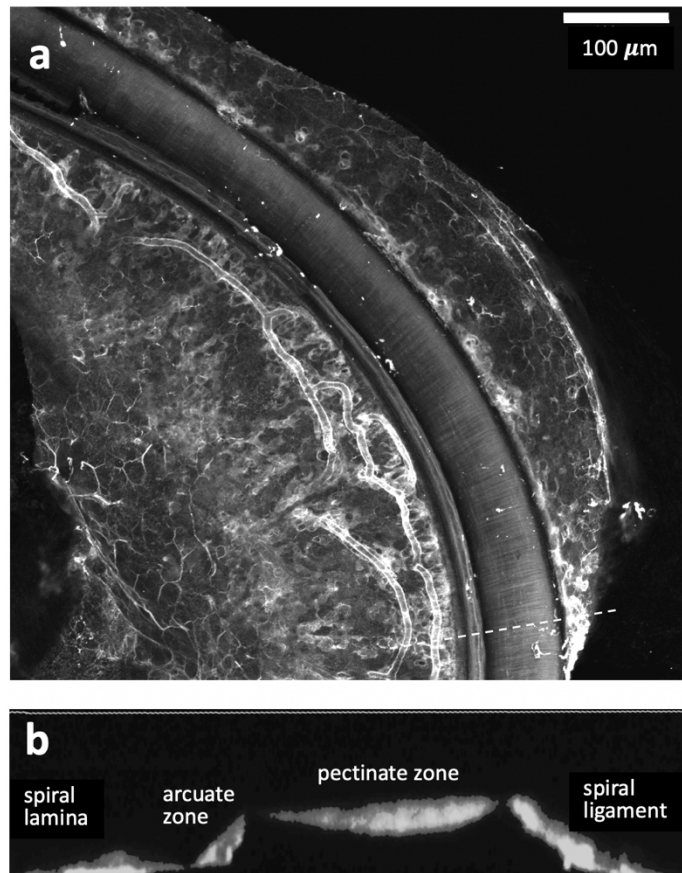
Figure 1 shows two examples of EP measured before, after and during scala media injections of 500 nL of PEG. Imaging from preparation g932 is in Figure 5 of the main article. The EP data of g928 is included to show a relatively long EP recording. This figure serves to demonstrate that the injections could be done without disrupting EP. During the injection there was some variation in the recorded EP which might have been due to vibration of the electrode when the injection pump was active. After the injection EP often increased slightly, perhaps due to a reduction in leakage paths in the somewhat inflated scala media.

Supplemental Figure 2.

Data supporting CNA35 penetration.

Mouse cochlea from the Columbia medical center animal facility. (The staining was for training purposes; the mouse was euthanized by facility staff and strain was not recorded.) Processing was like that for gerbil cochleae, with 2 hrs staining with CNA35-OG, followed by fixation, decalcification, dissection and imaging. TM had lifted off in this preparation. The preparation was imaged with scala tympani side facing imaging optics, and habenula perforata are therefore not imaged.

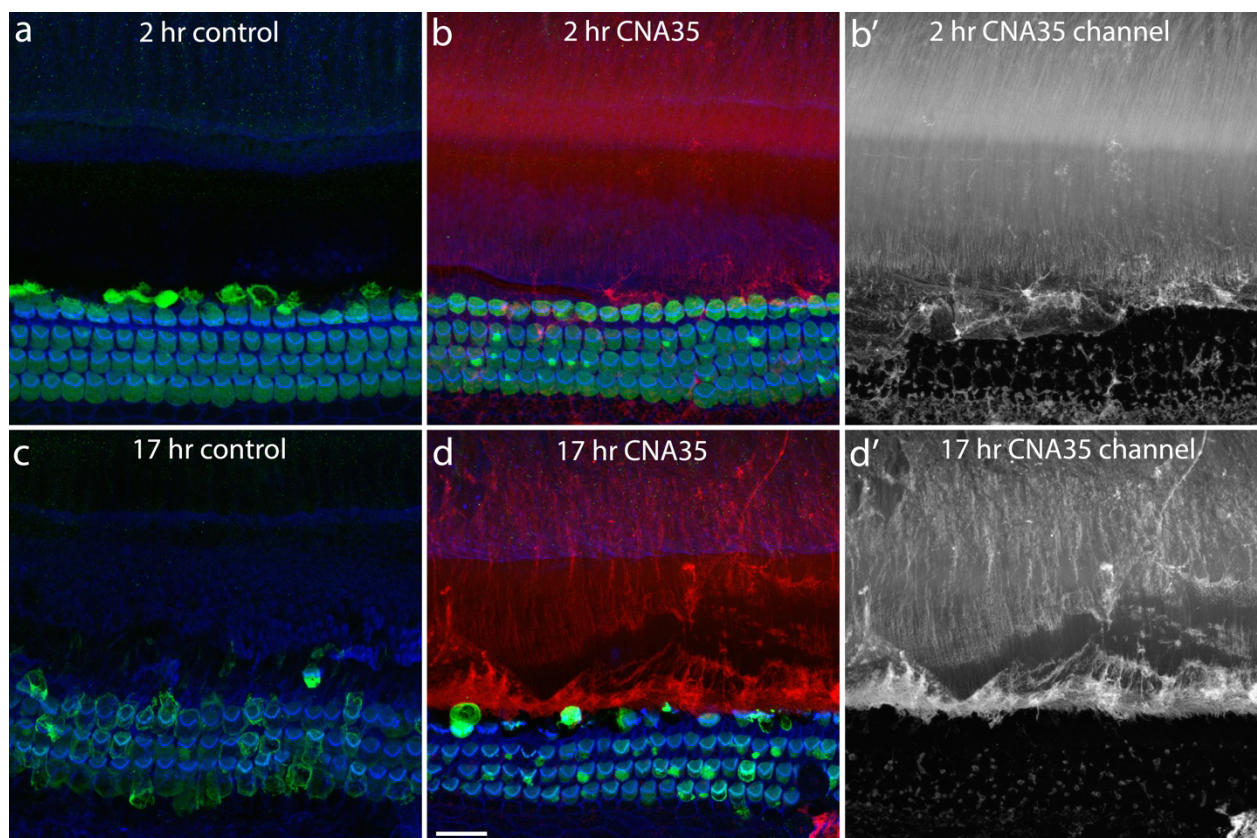
Fig. 2a. Radial-longitudinal view of BM. Maximum intensity projection of a Z-stack. Dashed line shows location of radial-transverse view in (b). b. Heat map radial-transverse view of BM. Lighter gray-shade corresponds to more intense staining. (a) shows BM radial fibrils, similar to the gerbil BM (for example, Fig. 3d), but the staining in the heat map in (b) shows a fibril distribution that is different than in gerbil. In this mouse cochlea collagen stained throughout the thickness of the BM with the most intense staining in the central area. This image is included to show that the CNA35 stain is able to penetrate the BM, and to support that the fibril banding observed in gerbil is not an artefact of poor penetration. Mouse 210721 slide 2.



Supplemental Figure 3.

Triple labeling exploration of the status of hair cells following CNA35 staining.

Figures 3-5 of the main paper showed CNA35 staining without any counterstaining of cellular tissues. The status of cells in those figures was unknown and surmised to be degraded because of the 2 hour or overnight incubation of unfixed tissue at room temperature in PBS. As a follow up, we stained P2 mouse cochlear cultures for either 2 hours (b, b') or 17 hours (d, d') at room temperature (~20°C) in PBS containing CNA35-Cy3 (red in supplemental Figure 3 b, d). The cultures were then washed briefly, fixed for 1 h in 3.7% formaldehyde, permeabilized with 0.1% TX-100 and counterstained with 633 phalloidin (Invitrogen) to label actin (blue) and rabbit anti-MYO7a (Proteus Biosciences) followed by AlexaFluor488 goat anti-rabbit (Invitrogen) to label hair cells (green). The control samples (a, c) were incubated in PBS at room temperature without CNA35 prior to fixation and staining. The figure shows that 2 hour incubated cultures have fairly normal looking hair bundles but variable abnormalities in the MYO7a staining of the cell bodies of the inner hair cells. The 17 hour cultures show more extreme degradation with clear signs of inner hair cell loss. There is no difference between the samples incubated with and without CNA35, thus there is no evidence that CNA35 is toxic to cells of the cochlea. Panels b' and d' show CNA35 staining alone from parts b and d respectively. Scale bar = 20 μ m.



35. Müller M (1996) The cochlear place-frequency map of the adult and developing mongolian gerbil. *Hear Res* 94:148–156
36. Müller M, von Hünerbein K, Hoidis S, Smolders JWT (2005) A physiological place-frequency map of the cochlea in the CBA/J mouse. *Hear Res* 202:63–73
37. Goodyear RJ, Richardson GP (2017) Structure, function, and development of the tectorial membrane: an extracellular matrix essential for hearing. *Curr Top Dev Biol* 130:217–224
38. Zhou W, Jabeen T, Sabha S, Becker J, Nam J-H (2022) Deiters cells act as mechanical equalizers for outer hair cells. *J Neuroscience* 42:8361–8372
39. Chan WX, Yoon Y-J (2015) Effects of basilar membrane arch and radial tension on the travelling wave in gerbil cochlea. *Hear Res* 327:136–142
40. Henson MM (1978) The basilar membrane of the bat, *Pteronotus p. parnellii*. *Am J Anat* 153:143–157
41. Yoon Y-J, Steele CR, Puria S (2011) Feed-forward and feed-backward amplification model from cochlear cytoarchitecture: an interspecies comparison. *Biophys J* 100:1–10
42. Meaud J, Grosh K (2010) The effect of tectorial membrane and basilar membrane longitudinal coupling in cochlear mechanics. *JASA* 127:1411–1421
43. Ghaffari R, Aranyosi AJ, Freeman DM (2007) Longitudinally propagating traveling waves of the mammalian tectorial membrane. *PNAS* 104:16510–16515
44. Olson ES, Mountain DC (1994) Mapping the cochlear partition's stiffness to its cellular architecture. *JASA* 95:395–400
45. Nosikova YS, Santerre JP, Grynopas M, Gibson G, Kandel RA (2012) Characterization of the annulus fibrosus-vertebral body interface: identification of new structural features. *J Anat* 221:577–589

Publisher's Note Springer Nature remains neutral with regard to jurisdictional claims in published maps and institutional affiliations.

Springer Nature or its licensor (e.g. a society or other partner) holds exclusive rights to this article under a publishing agreement with the author(s) or other rightsholder(s); author self-archiving of the accepted manuscript version of this article is solely governed by the terms of such publishing agreement and applicable law.